Journal of Thermal Science Vol.24, No.4 (2015) 303−312

DOI: 10.1007/s11630-015-0789-8 Article ID:1003-2169(2015)04-0303-10

Experimental Investigation of Effects of Suction-Side Squealer Tip Geometry on the Flow Field in a Large-scale Axial Compressor using SPIV

MA Hongwei*, WEI Wei, WANG Lixiang, TIAN Yangtao

1. Key Laboratory of Science and Technology on Aero-Engine Aero-Thermodynamics,
2 School of Energy and Power Engineering, Beihang University, Beijing, 100191, China
3 . Collaborative Innovation Center of Advanced Aero-Engine, Beijing, 100191, China

It is well known that the non-uniform tip geometry is a promising passive flow control technique in turbomachinery. However, detailed investigation of its effects on the unsteady flow field of turbomachinery is rare in the existing literatures. This paper presents an experimental investigation of effects of suction side squealer tip configuration on both the steady and unsteady flow field of an isolated compressor rotor. The flow field at 10% chord downstream from the trailing edge was measured using a mini five-hole probe. Meanwhile, the unsteady flow field inside the passage was investigated using stereo particle image velocimetry (SPIV). The steady results show that the SSQ tip configuration exerts positive effect on the static pressure rise performance of this compressor, and the radial equilibrium at the rotor outlet is obviously rearranged. The SSQ tip configuration would create a stronger tip leakage vortex at the formation phase, and it experiences a faster dissipation process around the rear chord. Also, the splitting process of the tip leakage vortex is severer, which is the main cause of the relatively higher probability of the presence of the streamwise reverse flow. The quantitatively analysis of the tip leakage vortex indicates that the velocity loss inside the blockage region is direct response of the evolutionary procedure of the tip leakage vortex. It keeps increasing until the end of the splitting process. Although the blockage coefficient grows sustainably, the velocity loss will reduce once the turbulent mixing procedure is dominant.

Keywords: tip leakage vortex, suction side squealer, axial compressor, SPIV, instantaneous flow field

Introduction

Generally, the loss related to the tip leakage flow could be divided into two categories, including the viscous effects within the tip gap, and mixing loss generated by the interaction between the leakage jet and the mainstream. Many targeted measures have been employed to reduce the detrimental effects induced by the leakage flow. Wadia and Booth [1-2] conducted a quantitive comparative experiment on three kinds of turbine cascade, and proposed a simple model to predict and minimize the tip flow. Bindon and Morphis [3] investigated the effects of rounded pressure side on the performance of a turbine cascade. The overall loss was almost unchanged; however, the internal loss was eliminated while the mixing loss was higher. But the experiment performed by them in a 1.5-stage turbine rotor showed that the efficiency was improved by using this kind of tip configuration [4]. Heyes et al. [5] conducted experiments on two turbine cascades, and they concluded that the performance of the

Received: March 2015 MA Hongwei: Professor
This study was co-supported by the National Natural Science Foundation of China (Grant No.51161130525/ No.51136003), the 111 Project (No.B07009)

Nomenclature

Z	streamwise direction
V_z	streamwise velocity
$V_{z,boundary}$	streamwise velocity on the boundary of the blockage area
L	Distance from the blade leading edge along the chordwise direction
C	Chord
RPM	rotational speed (r/min)
m_t	mass flow rate in one passage
A	domain of integration of blockage
Dp	dynamic pressure at inlet (Pa)
Ps	static pressure at outlet (Pa)
B_m	blockage coefficient of tip leakage flow
U_{tip}	tangential velocity of blade tip (m/s)
Cva	V_0 / U_{tip}, axial velocity coefficient at inlet
Cp	(Ps_1-Ps_0) /Dp, static pressure rise coefficient
Cvz	V_{a1} /U_{tip}, axial flow coefficient
r	radial direction

Abbreviations

PIV	Particle Image Velocimetry
SPIV	Stereo PIV
SS50/ SS90	50%/ 90% chord measurement slice
SSQ	suction side squealer tip geometry

Greek letters

ξ	relative total pressure loss coefficient normalized by Dp
λ_2	principle to identify the TLV
θ	circumferential direction

Subscripts

0	compressor inlet
1	compressor outlet
t	tangential
a	axial

suction-side squealer was improved more compared with the pressure-side squealer. They also proposed a model correlating the loss and the discharge coefficient, which confirmed that one should minimize the leakage mass flow at a given tip clearance rather than the loss generation over the tip. Denton [6] developed a tip loss model which shows several possible means of reducing tip leakage flow loss. Camci and Dey [7] performed an experimental investigation of aerodynamic performance of full and partial squealer rims in a turbine stage. The results show that the latter tip configuration exerted positive effects on the local aerodynamic field by means of weakening the tip leakage vortex. Such tip treatments could also be a promising measure to improve the heat transfer of the turbine blade tip [8–10].

The existing literature towards the application of this passive flow control technology in compressors is relatively less. Ma and Zhang [11] conducted an experimental investigation of flow field of one kind of grooved tip geometry. They suggested that the channel on the blade top smooths the pressure change across the blade, which prevents the formation of a clear and strong tip leakage vortex. The grooved tip increases the flow capacity at the incidence angles of 0 and 5 deg. However, it leads to more loss than the baseline at the two incidence angles, which is attributed to the larger loss within the tip gap while the mixing loss is reduced.

As known, the tip leakage also exerts profound effects on the stability of turbomachinery. Classic conclusion would be the almost linear relationship between the stall margin and tip clearance [12]. However, the influence of non-uniform tip clearance on the unsteady flow field is hardly known. Ghanem [13] investigated the unsteady leakage flow in a propeller using particle image velocimetry (PIV), and concluded that some changes of the flow variables have to be shifted and scaled to reveal the real unsteady flow features. Hong-Sik [14] performed a fully coupled fluid-structure interaction simulation in a multi-stage high pressure compressor, and found that the chordwise non-uniform tip clearance changed the dominant frequency of tip flow significantly.

Apart from the numerical simulation method, it is extremely difficult for the conventional experimental techniques to acquire the evolutionary procedure of the tip leakage flow inside the passage of a rotational turbomachinery. Most of the previous studies of the effects of non-uniform tip geometry on the flow field are conducted in cascades or at the exits of the rotor passage. Recently, the non-intrusive measurement techniques SPIV has been proved to be a promising tool to investigate the development of the tip leakage flow [15]. The creative experiment layout of SPIV in their test made it possible for the capture of the cross-sectional instantaneous tip leakage vortex. Yu [16] promoted this measurement technique to a higher level, and deliberately studied the kinematic and dynamic properties of the tip flow with variant flat tip configuration in a large-scale compressor. Zhang [17] investigated the relationship between the blockage induced by the tip flow and its evolutionary procedures in the same test facility.

The purposes of this paper are to present an experimental investigation on the effects of suction side squealer tip clearance in an isolated-rotor stage with multiple measurement techniques. And the evolutionary procedure of the tip leakage vortex is demonstrated quantitatively.

Experimental Procedure

Experimental Facility and Test Technique

The experimental investigation was carried out in a large-scale compressor facility (Figure 1) at Beihang University. An isolated rotor was deployed to provide the research environment. The compressor was operated at two operating points under the reduced rotational speed of 1100 RPM with a rotation speed drift of 1.0 RPM. The compressor casing is 1 m with a hub-to-tip ratio of 0.6. The isolated-rotor stage comprises 17 blades. The rotor blades with C4 airfoil are designed in terms of the free vortex law. The measurements were taken at the Reynolds number of 7.5e5 based on the blade chord and the inlet velocity. More details of the test rig refer to [18].

Fig. 1 The research isolated-rotor

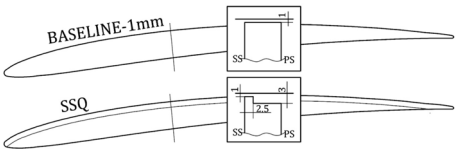

Fig. 2 The investigated tip clearances

The tip configurations explored include a flat tip (Baseline), and a suction side squealer tip (SSQ), as shown in figure 2. The case with the flat tip of 1 mm clearance is referenced as the baseline. The sectional views of tip configurations are also shown.

The boundary layers on both endwalls are about 3 mm and the inlet turbulence intensity is about 2%. The plane at 10% chord downstream from the rotor trailing edge was measured at 45 spanwise stations using a mini five-hole pressure probe. During the experiment, the flow capacity was kept as the invariant among the three tip configurations, which is obtained from a venturi tube at the inlet of the test rig. And it was also checked by computing the integral of *Cvz* from the data measured using the five-hole probe at the rotor outlet.

Calibration of the mini five-hole probe was carried out in a low-speed wind tunnel. The pitch angle and yaw angle range of calibration was ±28 degree and ±32 degree respectively, with an interval of 4 degree. Its uncertainties of angles are less than 1° while the uncertainty of total pressure is less than 1.0%. The uncertainty of all the pressure sensors deployed is less than 0.1% during a steady calibration.

The SPIV measurement system comes from LaVision Company. The device consists of two 12-bit 2048×2048 pixels Imager ProX4M CCD camera, Nd: YAG laser (140mJ/Pulse), PC, PTU, and Davis software. The maximum sampling frequency is 14 Hz, but in practice, the sampling frequency is limited to 7 Hz. The including angle between the two cameras is 120 degree as shown in Figure 3a.

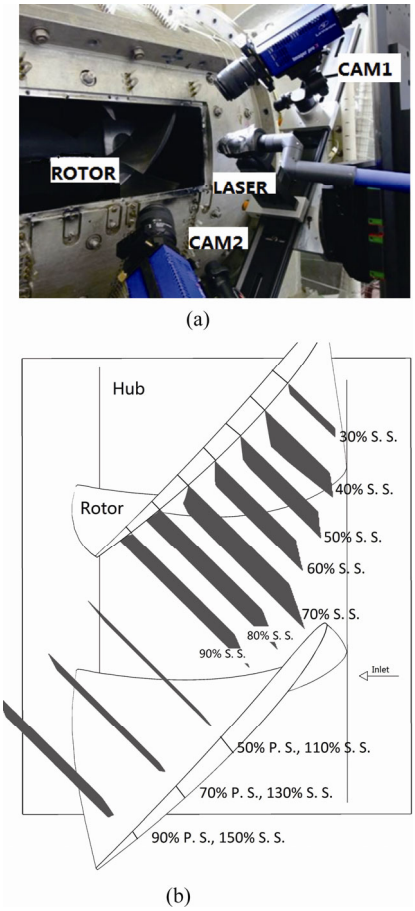

Fig. 3 Layout of SPIV test, (a) SPIV equipment, (b) the SPIV measurement slices

Ten slices were sampled during the experiment. The streamwise locations of the slices are shown in Figure 3b. Over 450 frames were averaged for each slice in the post processing. The multi-grid method is utilized to process each frame. The initial query window is 64×64, and the

final query window is 32×32. The corresponding physical space is about 1.5mm×1.5mm. Each slice is sampled by the double-frame double-exposure method. The average diameter of the particle is around 1 μm.

Result and Discussion

Overall Performance Comparison

Performance map of the compressor is plotted in figure 4 by the static pressure rise coefficient versus the axial velocity coefficient. A slight improvement could be observed throughout the operation while the SSQ tip configuration is applied.

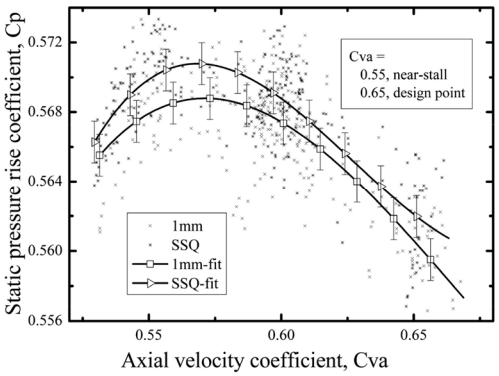

Fig. 4 Compressor performance map

Figure 5 illustrates the spanwise integral mass averaged relative total pressure loss derived from five-hole probe result. The definition is given by

$$\xi = \sum_{Root}^{Tip}\left[(\frac{1}{2}\rho V_{a,in}^2 + P_{S,in} + \frac{1}{2}\rho U_{Span}^2) - (\frac{1}{2}\rho W_2^2 + P_{S,out})\right] / D_P \quad (1)$$

where U_{span} gives the spanwise distribution of tangential velocity of the rotor blade.

It is effective to reduce the relative total pressure loss with SSQ as shown in figure 5. Peak loss reduction locates at the near-stall point. According to the definition given, the uncertainty of massflow averaged relative total pressure loss is 2.8E-3 (5.1% of the baseline loss) which is mainly attributed to the uncertainty of Ps, out (~8 Pa). Considering the small variation of relative total pressure loss between the two cases as well as the slight change of the performance, a preliminary conclusion could be drew that the modification in the tip would not exert profound influence on the steady flow field in this large-scale facility.

Although the improvement of the integral parameters is not obvious, the spanwise distribution of other flow parameters have been rearranged obviously as shown in figure 6. 'SSQ minus Baseline' labelled in figure 6b means the difference of the relative flow angle between the SSQ and baseline. Typically, in the tip region, the spanwise distribution of flow capacity and relative flow angle indicates that the tip leakage flow is pushed away from the suction side slightly. In the meantime, the flow capacity is also improved. The variation induced by the tip reform is clearly larger than the measurement error, which is credible.

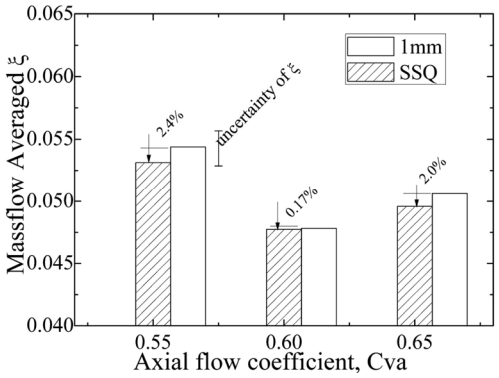

Fig. 5 Mass-averaged relative total pressure loss comparison

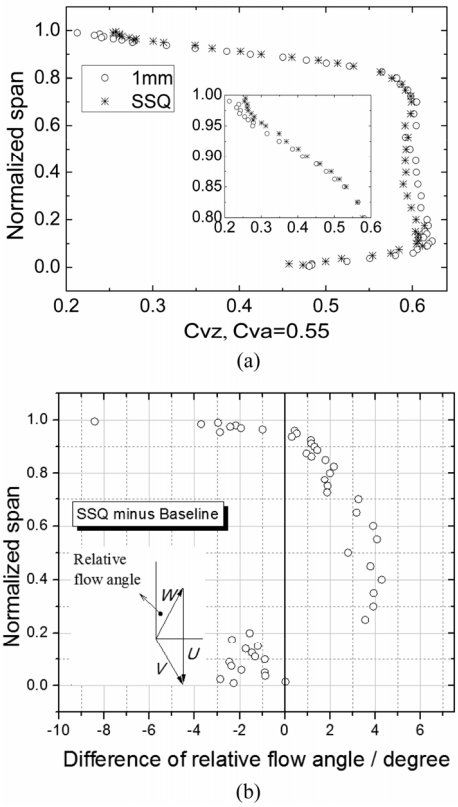

Fig. 6 Spanwise distribution and variation of (a) flow capacity, (b) relative flow angle, *Cva* = 0.55

Considering this comparison experiment is carried out under the invariant of massflow rate, the flow capacity below 80% span is decreased consequently, especially in the hub region. However, the distribution pattern of the variation of *Cvz* below 80% blade height could be identified as relative uniform offset, while the tip region fol-

lows a monotone increasing pattern. In another word, the radial distribution of loading is changed due to the slightly variation of radial equilibrium. The test facility is designed under the hub-shroud-ratio of 0.6, which is a relative low value in the modern compressor design. And it is believed to be the reason for the sensitive correlation between the tip region and the main stream.

Time-averaged Flow Field inside the Passage

Figure 7 and figure 8 respectively illustrate the ensemble-averaged streamwise velocity which is normalized by the rotor tip velocity at two operational points. The low-velocity region of the tip leakage flow is larger with the SSQ tip configuration than the one with the baseline at both conditions. This is especially clear at 70% to 110% chord measurement slices (SS70–SS110). However, this difference is unclear at the rotor exit.

In order to quantitatively evaluate the blockage caused by the two tip configurations, a blockage coefficient of the tip leakage flow is defined in the equation (2). The domain of integration A is the area that affected by the tip leakage flow in the tip region. This definition takes the variation of streamwise velocity into account, and it has been verified by Yu and Zhang et al. [refs].

$$B_m = \int_0^A (\rho V_{z,boundary} - \rho V_z) dA / m_t \tag{2}$$

where $V_{z,boundary}$ is the streamwise velocity on the boundary of the blockage area, and m_t is the massflowrate in one passage. The blockage coefficient of the tip leakage flow is shown in figure 9.

The blockage develops quite linearly at the first several slices. According to the evolution theory proposed by Yu [16] and Zhang [17], the blockage is strongly associated with the development of tip leakage vortex. The rapid increase of blockage is mainly induced by the destabilization of the tip leakage vortex, and this pattern will reverse while the turbulent mixing process is dominant.

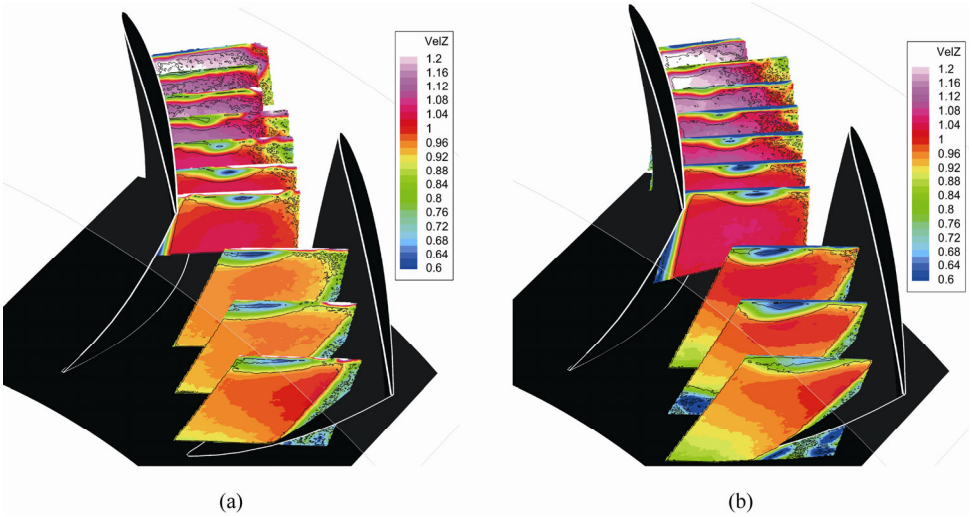

Fig. 7 Ensemble-averaged streamwise velocity, design point, normalized with the rotor tip velocity (a) Baseline, (b) SSQ

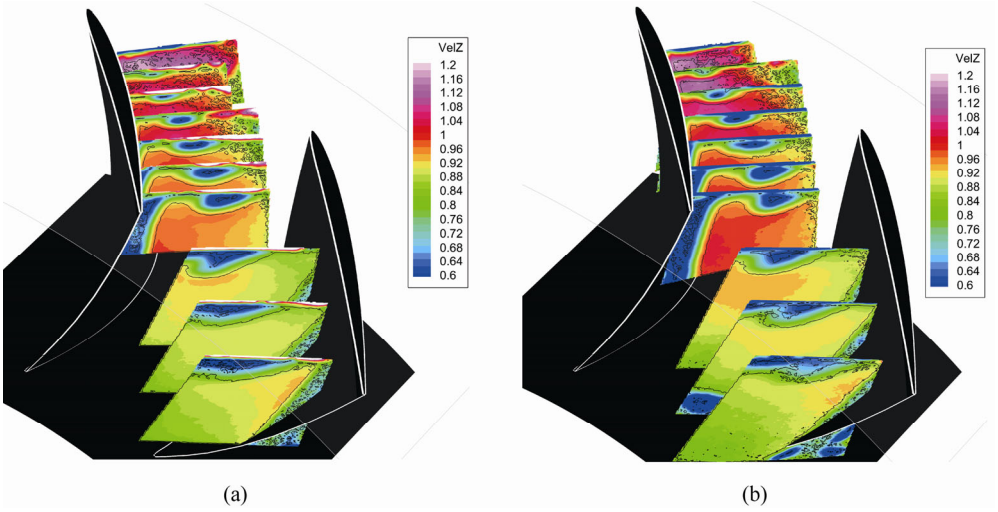

Fig. 8 Ensemble-averaged streamwise velocity, near-stall, normalized with the rotor tip velocity (a) Baseline, (b) SSQ

The SSQ tip configuration obviously leads to a larger blockage effect at both of the operational points, which could also be attested in figure 7 and figure 8. At the rear locations, the difference is smaller. It seems a stronger tip leakage vortex is induced by the SSQ tip configuration.

Figure 10 shows the velocity loss of the tip leakage flow comparing with the mainstream, and a similar pattern is observed. The velocity loss increases at the first several slices, but the loss will decrease in advance of the blockage. This is because the velocity loss directly represents the status of the tip leakage vortex.

The bold line segment in figure 10 indicates the start of the splitting process, and the peak of velocity loss means that the splitting process is almost finished around SS70 measurement slice. This will be demonstrated and discussed in the next section.

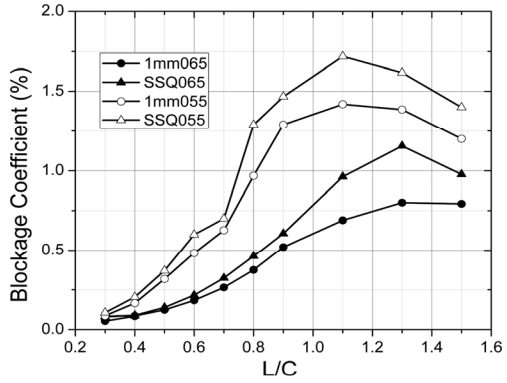

Fig. 9 Blockage coefficient of the tip leakage flow

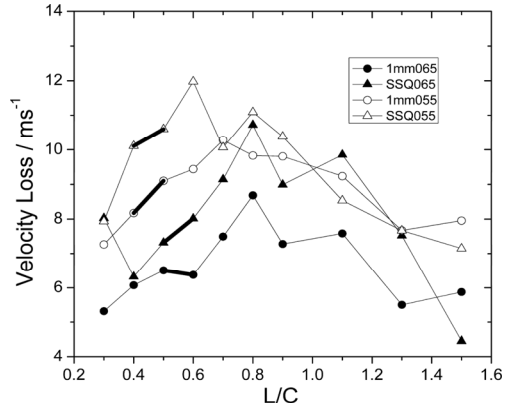

Fig. 10 Velocity loss of the tip leakage flow

At the rotor outlet, the velocity loss induced by the SSQ tip configuration is smaller than the baseline, which is in accord with the steady measurement taken by the five-hole probe.

Several preliminary conclusions could be drawn that 1) the blockage represent the integration effects of the streamwise velocity loss, 2) the velocity loss is a direct response of the evolutionary procedure of the tip leakage vortex, 3) the SSQ tip configuration would create a stronger tip leakage vortex at the formation phase, and it experiences a faster dissipation process in the rear chord region.

Instantaneous Flow Field in the Tip Region

In order to investigate the instantaneous flow field in the tip region, a vortex identification program using the λ_2 principle was developed to locate the tip leakage vortex. The definition is given by equation (3), which is a simplified -λ_2 principle.

$$\lambda_2 = (\frac{\partial V_r}{\partial r})^2 + (\frac{\partial V_\theta}{r\partial \theta})^2 + 2 \cdot \frac{\partial V_r}{r\partial \theta} \frac{\partial V_\theta}{\partial r} \tag{3}$$

Due to the lack of the gradient of the streamwise velocity in the SPIV measurement, some classic principles to identify vortices are no longer practicable, including Q, -λ_2, Δ principle. This simplified principle has been attested to be accurate and effective to identify the tip leakage vortex core [15].

The program is coded with MATLAB, and the data source is the instantaneous frames extracted from the Davis software. The main function of the program includes the following parts, 1) identification and elimination of the pseudo vectors; 2) ensemble-averaged calculation of the sampled frames; 3) identification of the tip leakage vortex core; 4) orientation of the vortex core boundary; 5) location, circulation and radius calculation of the vortex core. It has to be mentioned that only the blockage region is investigated to rule out the small flow disturbance in the main stream. This threshold of λ_2 is zero to strictly rule out the useless information.

Figure 11 shows the time-averaged and instantaneous flow fields of identified vortices at the 50% S. S. and 90% S. S. measurement slices (SS50, SS90) while the baseline tip geometry is applied. The horizontal axis is the normalized span, and the vertical axis is the normalized distance between the local positions to the suction surface. The center of the tip leakage core is marked with a white five-pointed star, and the blue solid line is the identified boundary of the core. The black dash line is the fitting ellipse of the boundary of the core. The black dots on the background indicate the centroids of query window array.

The first plot of figure 11a and the first plot of figure 11b are the time-averaged results. Both of them show a clear tip leakage vortex structure with concentrated negative vorticity. Nevertheless, the instantaneous flow fields which are randomly chosen from the database show a completely different pattern. The size, strength, and location of the identified tip leakage vortex is time-varying. Even at SS50 measurement slice, the tip leakage vortex is not concentrated as the time-averaged data. At SS90 measurement slice the tip leakage vortex is scattered. It could be concluded that the time-averaged results obtained with SPIV cover plenty of unsteady characteristics of the tip leakage flow.

In order to evaluate the unsteady characteristics of the tip leakage vortex, a statistical approach is applied to investigate its evolutionary procedure. The method is proposed by Ghanem [13], and it is quite an effective and clear way to research the unsteady properties of this singular flow structure.

The data of each identified vortex extracted in every instantaneous flow field is gathered into one database to calculate the statistical properties of the vortices. Figure 12 shows the histogram of several parameters extracted from the instantaneous flow fields at the first five measurement slices while the compressor is operated in the design point. The vertical axis indicates the probability of the data in the histogram, and the horizontal axis represents the value of the parameters. And figure 13 shows the same plot while the compressor is working in the near stall situation.

As shown in the left column of figure 12, the radial locations of the identified vortices of the two tip configurations are quite similar. However, the circumferential position of the vortices is pushed further from the suction surface while SSQ is applied.

Comparing the circulation among the five slices, it could be seen that the circulation clearly decreases to a lower level in both of the tip configurations. In SS70 measurement slice, the identified vortex core is much smaller and weaker than the SS30 measurement slice. The corresponding physical phenomena are the splitting process of the tip leakage vortex under a strong negative pressure gradient. Similarly, the radius of the vortex core is also smaller.

The identified vortices are getting decentralized while the tip leakage vortex is developing downstream. The displacement between the center of the time-averaged data and the ones in the instantaneous flow field increase rapidly. It could be seen in the right column of figure 10 that the small vortex cores uniformly distribute in the blockage area at the SS70 measurement slice.

The splitting of the tip leakage vortex core starts at SS40 measurement slice after which the circulation distribution is moving towards the small value. At SS70 measurement slice, the splitting process of the tip leakage core has almost finished, and the turbulent mixing process is dominant in the development of the tip leakage flow.

As discussed in the literature [16, 17], and also considering the quantitive analysis of the instantaneous flow field above, a clear development process of the tip lea-

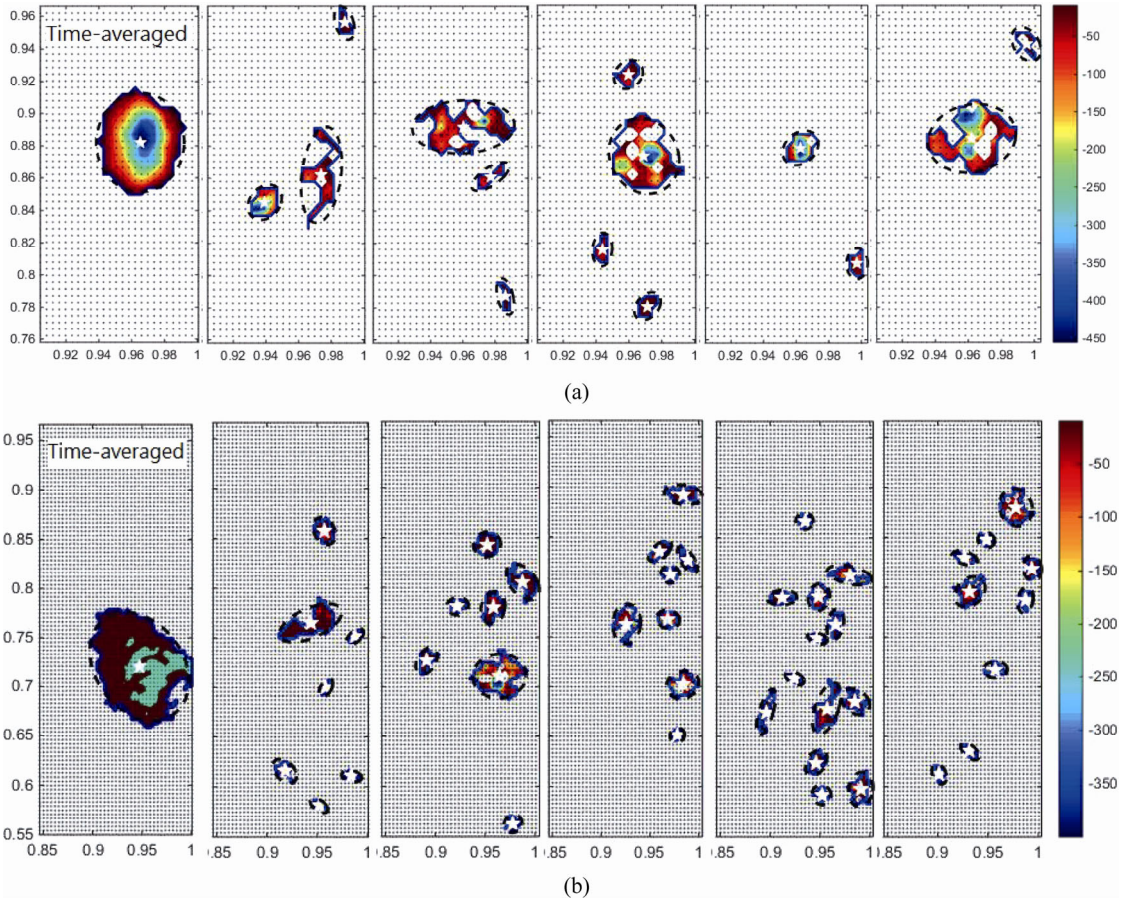

Fig. 11 Time-averaged and instantaneous flow fields of identified vortices at (a) SS50 (b) SS90

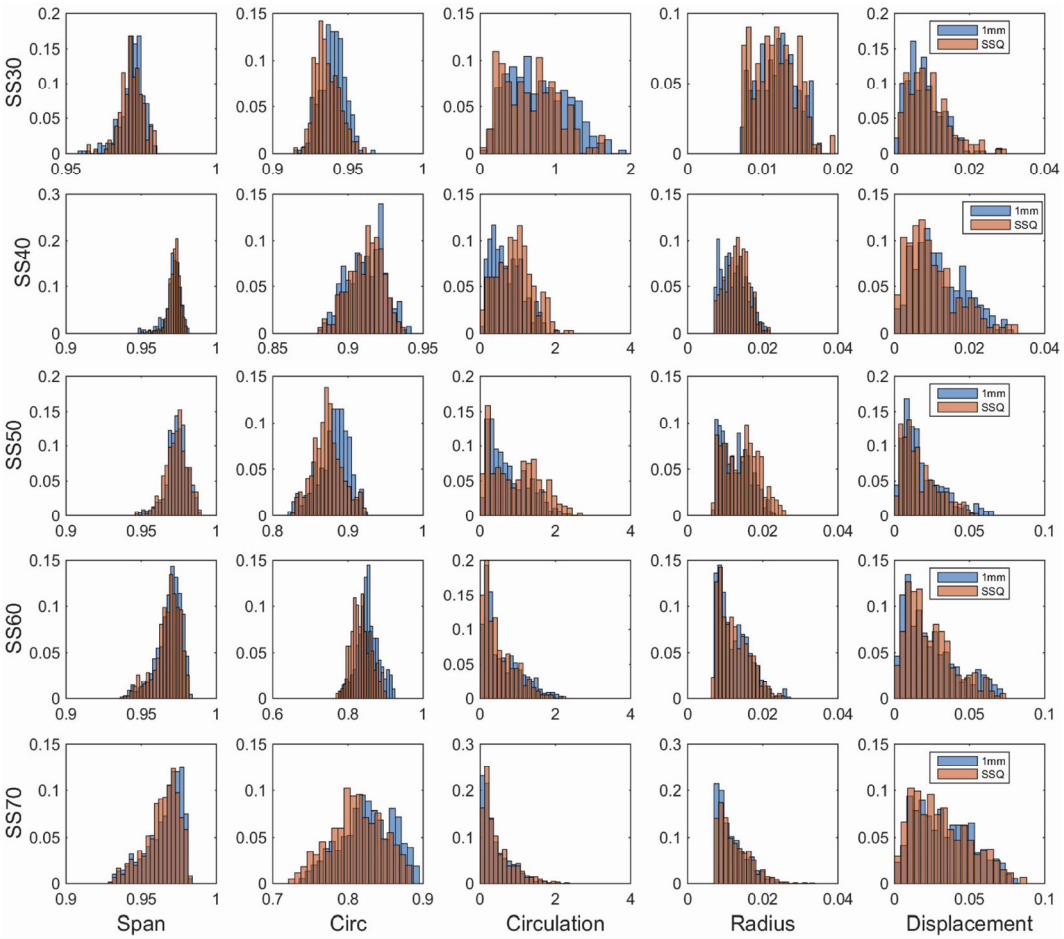

Fig. 12 Statistics of the instantaneous flow fields at five different measurement slices, design point

kage vortex could be obtained at the design point as the following: 1) the formation of the leakage flow, 2) the split process due to the strong negative pressure gradient, 3) the turbulent mixing process.

As for the SSQ configuration, it obviously leads a strong effect towards the tip leakage flow. It is believed that the larger curvature of the squealer should be responsible for a stronger tip leakage vortex, and consequently give rise to larger radius and circulation of the tip leakage vortex core at the first three slices. However, due to the smaller supplement of flow at the rear chord, its splitting process is faster than the baseline.

Comparing with the development shown in figure 12, the plot in figure 13 shows a similar pattern. But the splitting process is much faster due to the severer negative pressure gradient, as a result, the size and strength of each small vortex core decrease faster than that in design point. This is a quite different conclusion with that obtained from the time-averaged results.

The discussion above also proves the conclusion that obtained through the figure 9 and figure 10. The velocity loss in the blockage region is strongly associates with the evolutionary procedure of the tip leakage flow. The velocity loss keeps increasing until the end of the splitting process, and it will reduce once the turbulent mixing procedure is dominant. In the turbulent mixing process, the blockage however will still increase.

Figure 14 shows the numbers of identified vortex cores per effective frame. The vortex splitting is almost linearly developing throughout the evolutionary procedure of the tip leakage vortex. It has to mention that the number of the vortex core is less than 1 at SS30 measurement slice. It attests that the tip leakage vortex is not always exists at the very beginning of the formation process. The roll-up of the tip leakage vortex is intermittent due to the severe surrounding environment. The splitting process induced by SSQ tip configuration is more severe in both the operating conditions, which shows a similar trend with the development of blockage observed in figure 7 and figure 8.

The negative pressure gradient is much larger while the compressor is operated at the near stall condition. The tip leakage vortex will also experience a different evolution procedure with the design point. As shown in figure

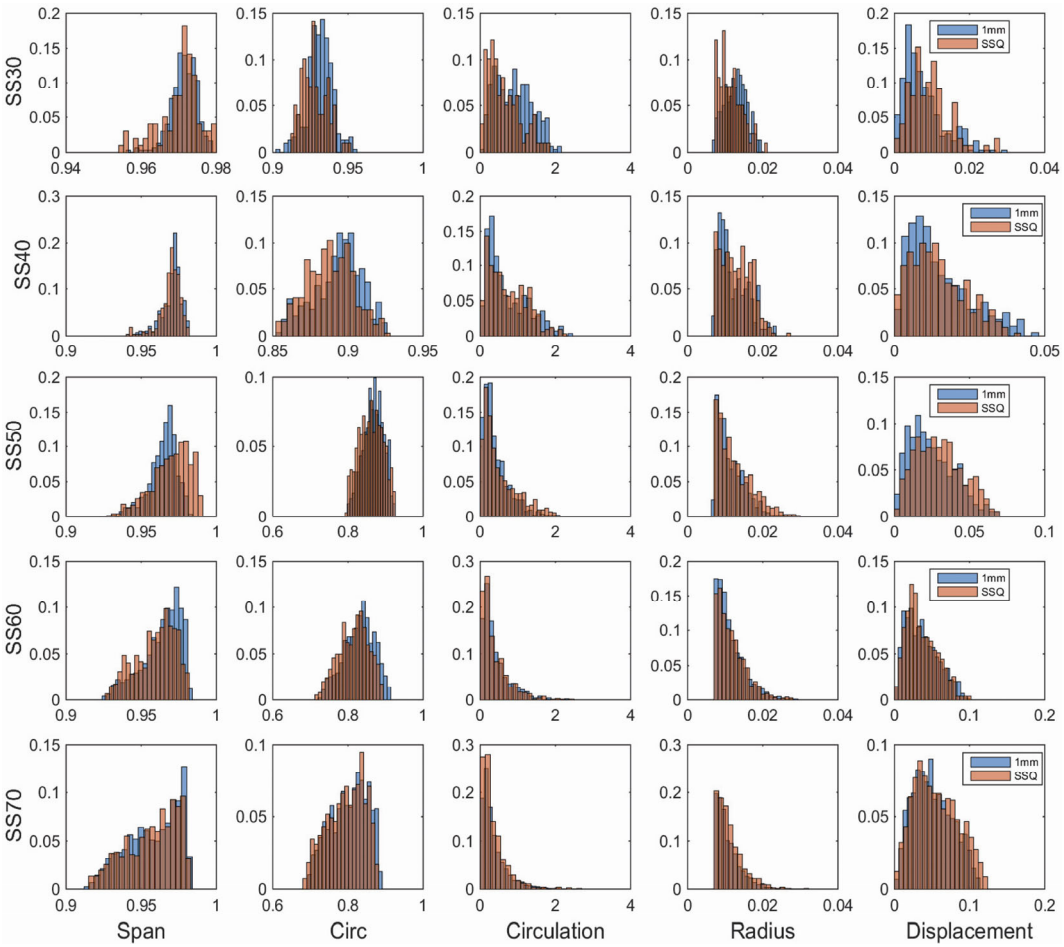

Fig. 13 Statistics of the instantaneous flow fields at five different measurement slices, near stall

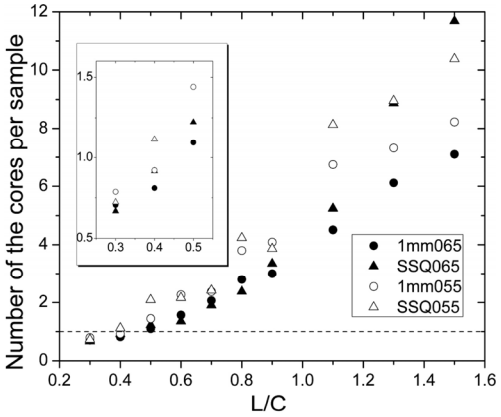

Fig. 14 Numbers of the identified vortices per effect frame

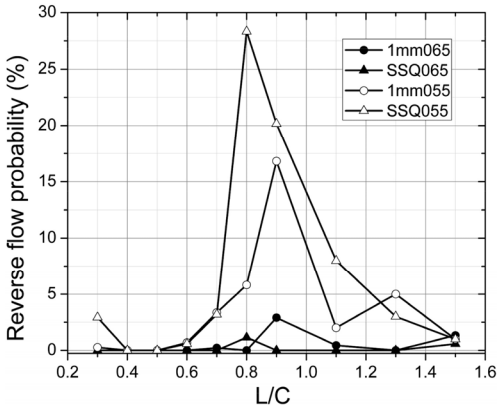

Fig. 15 Probability of the occurrence of the reverse flow in the tip leakage region

15, there exists much greater probability of the presence of the reverse flow in the tip leakage region. The SSQ tip configuration would experience a more severe destabilization process than the baseline, which could be attributed to the stronger tip leakage vortex and less supplement of flow at the rear chord.

Conclusions

This paper presents a detailed experimental investigation of the effects of two tip configurations on the flow field of an isolated compressor rotor. Several conclusions are summarized as following.

(1) The SSQ tip configuration exerts positive effect on the static pressure rise performance of this compressor. However, considering the measurement uncertainty, its influence on the steady flow field is mainly limited to the radial equilibrium at the rotor outlet rather than the total performance.

(2) From the viewpoint of time-mean flow field, the SSQ tip configuration would create a stronger tip leakage vortex at the formation phase, and it experiences a faster dissipation process in the rear chord region. The analysis of the instantaneous flow field shows that the splitting process of the tip leakage vortex is more severe while the SSQ tip configuration is applied. Meanwhile, the probability of the presence of the reverse flow is relatively larger due to the stronger destabilization process.

(3) The blockage coefficient represents the integration effects of the streamwise velocity loss, and the velocity loss is a direct response of the evolutionary procedure of the tip leakage vortex. The velocity loss in the blockage region keeps increasing until the end of the splitting process. Although the blockage grows sustainably even in the turbulent mixing phase, the velocity loss will reduce once the turbulent mixing procedure is dominant.

(4) The number of identified vortex core is less than 1 at the first measurement slice. It attests that the tip leakage vortex is not always exists at the very beginning of the formation process. The roll-up of the tip leakage vortex is intermittent due to the severe surrounding environment.

Acknowledgement

The authors would like to thank YU Xianjun and AN Guangfeng for their critical and constructive review of the manuscript. This study was co-supported by the National Natural Science Foundation of China (Grant No.51161130525/ No.51136003), the 111 Project (No.B07009), and the Innovation Foundation of BUAA for PhD Graduates (No.YWF-14-YJSY-014).

References

[1] Booth, T. C., Dodge, P. R., and Hepworth, H. K., Rotor-Tip Leakage: Part I-Basic Methodology, ASME Paper 1981 No. 81-GT-71, March 9-12, Houston, Texas, USA.

[2] Wadia, A. R., and Booth, T. C., Rotor-Tip Leakage: Part II-Design Optimization through Viscous Analysis and Ex-periment, ASME Paper No. 1981-GT-72, March 9−12, Houston, Texas, USA.

[3] Bindon, J. P, and Morphis, G., The Development of Axial Turbine Leakage Loss for Two Profiled Tip Geometries Using Linear Cascade Data, ASME J. Turbomachinery., 1992, 114: 198−203.

[4] Morphis, G., and Bindon, J. P., The Performance of a Low Speed One and A Half Stage Axial Turbine with Varying Rotor Tip Clearance and Tip Gap Geometry, ASME Paper No. 1994-GT-481, June 13−16, The Hague, Netherlands.

[5] Heyes, F. J. G., Hodson, H. P., and Dailey, G. M., The Effect of Blade Tip Geometry on the Tip Leakage Flow in Axial Turbine Cascades, ASME J. Turbomach., 1992, 114: 643−651.

[6] Denton, J.D., Loss Mechanisms in Turbomachines, ASME J. Turbomachin.,1993, 115: 621−656

[7] Camci, C., Dey, D., and Levent, K., Tip Leakage Flows near Partial Squealer Rims in an Axial Flow Turbine Stage, ASME Paper No. GT2003-38979, June 16−19, Atlanta, Georgia, USA.

[8] Ameri, A. A., Heat Transfer and Flow on the Blade Tip of a Gas Turbine Equipped With a Mean-Camberline Strip, ASME J. Turbomach., 2001, 123: 704−708.

[9] Sumanta, A., Numerical Study of Flow and Heat Transfer on a Blade Tip with Different Leakage Reduction Strategies, ASME Paper No. GT2003-38617, June 16−19, Atlanta, Georgia, USA.

[10] Saha, A. K. Sumanta, A. Chander, P., and Ron, B., Blade Tip Leakage Flow and Heat Transfer with Pressure-Side Winglet, ASME Paper No. GT2003-38620, June 16−19, Atlanta, Georgia, USA.

[11] MA Hongwei, ZHANG Jun, ZHANG Jinghui, YUAN Zhou, Experimental Study of Effects of Grooved Tip Clearances on the Flow Field in a Compressor Cascade Passage, ASME J. Turbomach., 2012, 134: 051012.

[12] Baghdadi S., Modeling Tip Clearance Effects in Multistage Axial compressors, ASME J. Turbomachin., 1996, 118(4): 613−843.

[13] Ghanem F.O., Steven L.C., Instantaneous and time averaged flow fields of multiple vortices in the tip region of a ducted propulsor, Exp. in Fluids, 2005, 38: 615−636.

[14] Hong-Sik Im, Ge-Cheng Zha, Effects of rotor tip clearance on tip clearance flow potentially leading to NSV in an axial compressor, ASME Turbo Expo 2012, GT 2012-68148, June 11−15, Copenhagen, Denmark.

[15] LIU Baojie, YU Xianjun, YUAN H. J., LIU H. X., JIANG H. K., and XU Y. T., Application of SPIV in Turbomachinery, Exp. Fluids, 2006, 40(4): 621−642.

[16] YU Xianjun, Experimental Investigations and Approximate Analyses for the Three-Dimensional Flow Fields in the Endwall Region in a Subsonic Axial Compressor Stage, PhD Dissertation, Beihang University, 2007.

[17] ZHANG Zhibo, Investigation and Approximate Analyses for the Tip Leakage Flow in the Subsonic Axial Compressor Stage, PhD Dissertation, Beihang University, 2013.

[18] MA Hongwei, WEI Wei, Experimental Investigation of Effects of Distributed Riblets on the Aerodynamic Performance of a Low-speed Compressor, J. Thermal Science 2013, 22(6): 592−599.